Effect of the concentration of MAPA on the heat of absorption of CO_2 and on the cyclic capacity in DEEA-MAPA blends

Hanna K. Knuutila*, Åsne Nannestad

Norwegian University of Science and Technology, 7491 Trondheim, Norway

Highlights:

- The effect of amine concentration on the heat of absorption of CO_2 is studied and discussed
- Equilibrium pressure of CO_2 and the heat of absorption is reported up to 120°C.
- Using equilibrium data, the cyclic capacity of the studied systems is calculated.

Abstract

In this work, the heat of absorption of CO_2 in aqueous blends of 2-(diethylamino)ethanol (DEEA) and 3-(methylamino)propylamine (MAPA) were measured as a function of CO_2 loading at 40°C, 80°C and 120°C. The main objective was to investigate the effect of concentration of MAPA on the heat of absorption. Furthermore, from the total pressure measurements the partial pressure of CO_2 was estimated and cyclic capacities were calculated. The study included systems forming one and two liquid phases during CO_2 absorption. The results show that increasing the concentration of MAPA in a 3M DEEA solution raised the heat of absorption at all temperatures. Similarly the cyclic capacity increased with the rise of MAPA content in 3M DEEA blends. However, increasing the MAPA concentration up to 5M and simultaneously decreasing the DEEA concentration to 1M, decreased the cyclic capacity.

1. Introduction

CO_2 removal from the gas stream using chemical absorption is a commercial technology. One of the main challenges with this technology is the energy consumption of the process. Thus,

* *Corresponding author. Tel.: +47 73594119; fax: +47 735 94080.*
E-mail address: hanna.knuutila@ntnu.no

over the last two decades substantial efforts have been focused on developing new absorption solvents with better properties. The energy requirement in the CO_2 absorption process is basically subject to three sources, i) the heat to overcome the sensible heat loss when recycling the solvent system between two temperatures, ii) the heat required to produce the stripping steam needed for obtaining the regenerator overhead total pressure (in addition to CO_2), and iii) the heat to reverse the absorption reaction. Much emphasis has been put on how to reduce the sensible heat loss (low circulation rate, high capacity) and the need for stripping steam (high temperature sensitivity and higher stripping temperature). For primary amines, e.g. MEA, the heat of reaction is around 83-85 kJ/mol CO_2 absorbed (Kim et al., 2014), equivalent of about 2 GJ/ton CO_2 energy requirement in a post combustion CO_2 capture process.

Over the years, many solvents have been proposed and studied. Among them are so-called de-mixing solvents. One example is 5M 2-(diethylamino)ethanol (DEEA) + 2M 3-(methylamino)propylamine (MAPA) –system, which separates into two liquid phases upon being loaded with CO_2, one phase being lean in CO_2, the other very rich in CO_2 (Arshad et al., 2013; Liebenthal et al., 2013; Pinto et al., 2014b). In the blend, DEEA is a tertiary alkanolamine with a low heat of absorption and MAPA has two amine functional groups, primary and secondary, that increase the heat of absorption (Arshad et al., 2013). At the same time since MAPA is a diamine, high CO_2 loadings can be attained with low pressures of CO_2. Furthermore, MAPA absorbs CO_2 faster compared than DEEA (Monteiro et al., 2015; Monteiro et al., 2013). In the case of the 5M DEEA+2M MAPA –system, the idea is to strip only the rich phase, thereby reducing the circulation rate, and benefiting from the high CO_2 content to obtain very high CO_2 pressure during stripping. This either produces CO_2 at elevated pressures or takes advantage of the good temperature sensitivity to regenerate at low temperatures. Potentially the system operates in a loading range where the average heat of reaction is between that of primary and tertiary amines, thus reducing the heat of absorption from 2 to about 1.5 GJ/ton CO_2 (Liebenthal et al., 2013). A pilot study of the two liquid phase forming systems confirmed the potential for low total heat requirements as specific heat demands below 2.4 GJ/ton CO_2 were obtained (Pinto et al., 2014a).

As discussed above, the heat of absorption is an important parameter when designing new solvent systems. Furthermore as discussed by Kim et al. (2011), the heat of absorption, the sum of heat of dissolution and the heat of reaction, increases with temperature and the absorption capacity decreases with increasing temperature. The effect of the amine concentration on the heat of absorption in a single amine system has been discussed in several publications (Arshad et al., 2013; Kim and Svendsen, 2011; Merkley et al., 1986). In the latest publication Arshad

et al. (2013) proposed further investigations to see the effect of the amine concentration. However, no data are available that relate to a systematic study of the differential heat of absorption of CO_2 into amine blends with varying amine ratios.

Thus in this work, the heat of absorption of CO_2 with aqueous mixtures of DEEA and MAPA are measured as functions of loading, temperature, and the MAPA concentration. Even though the main focus is on the effect of the MAPA concentration on the heat of absorption, the absorption capacities of the studied systems are also briefly discussed.

2. Experimental methods and procedures

In this work, 2-(diethylamino)-ethanol (DEEA, CAS 100-37-8) with purity 99.5%, 3-(methylamino)-propylamine (MAPA, CAS 6291-84-5) with purity 98% and CO_2 (purity 99.99%) were used without further purification. Aqueous solutions were prepared by gravimetrically using distilled de-ionized water.

The experiments were performed using two similar reaction calorimeters CPA-122 (Chemisens). Figure 1 presents the setup. *Calorimeter 1* shown in Figure 1 has been previously used by several authors (Arshad et al., 2013; Jonassen et al., 2014; Kim et al., 2014; Kim and Svendsen, 2007; Liu et al., 2012). The procedures used in this work are the same as in (Kim et al., 2014) for both calorimeters. A total of 25 experiments were performed using *Calorimeter 2* and four with C*alorimeter 1*.

The calorimeters are jacketed reactors with 2000 cm^3 volume, mechanically agitated that can measure the heat flow in the system, the temperature and total pressure as a function of time. The reactors were operated at isothermal conditions. CO_2 was added from the CO_2-cylinders and through a mass flow controller. This made it possible to calculate the added CO_2 both based on pressure change and temperature in the cylinders as well as the measured flow though the mass flow controller. Pt100 temperature sensors (accuracy ±0.1 K at 273 K, ±0.027 K at 373 K) were used to measure the temperature in the reactors and pressure transducers OMEGA (0-10 bara, 0.15% FS) were used to measure the pressure in the reactors. Calorimetric sensitivity given by the producer is 0.1 W. Finally temperature, pressure, heat flow and other operation parameters were recorded at 10 sec intervals.

Since the experimental procedures and data treatment used in this work are the same as in (Kim et al., 2014) only a brief description is given here. Each experiment was started by degassed under vacuum the reactor down to ~0.03 bara. After that a known amount liquid (approximately 1.3 L) was added into the reactor using a feed bottle weighed before and after

liquid feeding. The reactor was again evacuated to remove the air and de-gas the solution. The temperature was set and the stirrer was started. After the system reached equilibrium, CO_2 was added through a bottom valve and the heat removed was measured. After equilibrium was reached a new batch of CO_2 was added. The amount of CO_2 added to the reactor was calculated in two ways: 1) integration of the CO_2 flow over time, measured by the flow-controller, and 2) calculations with the Peng-Robinson equation of state using information about the pressure difference and temperature in the CO_2 cylinders. The average difference between these methods was $\pm 0.01 mol_{CO2}/mol_{amine}$ in loading. The results given in this work are based on the pressure and temperature in the CO_2 cylinders and the Peng-Robinson equation.

As in Kim et al. (2014) the total pressure data were used to calculate the equilibrium partial pressure of CO_2 at each loading. The assumption used was that partial pressure of (amine + water) remains constant during the experiment and is equal to the total pressure in the reactor before the first addition of CO_2 (Kim et al., 2014). Care should be taken when using the partial pressure of CO_2 at low loading and consequently at low total pressures. First, the approach used can lead to high relative errors at low partial pressures of CO_2 since two very similar numbers, the total pressure with CO_2 and pressure before adding CO_2, are subtracted from each other. At 40°C and CO_2 partial pressure of around 5kPa, a mistake of 1kPa in the measurement of the total pressure before adding CO_2 (~40kPa) would lead in a relative error of 20%. Second, the accuracy of the pressure transducer was 1.5 kPa, indicating that partial pressures below that have high inaccuracy. Nevertheless, the CO_2 partial pressure data gathered in this work are very consistent.

Arshad et al. (2013) used the same equipment and methodology and estimated the uncertainty of the heat of absorption measurement to be 2.1%. In the current work, 13 experiments were performed twice. In order to better understand the repeatability, a polynomial curve was fitted using the data points for the experiments performed in this work. Then the average deviation (AD) as well as the average standard deviation (AARD) between the measured points (x_i) and the fitted curves (x_{curve}) were calculated using the equations below:

$$\mathrm{AD} = \frac{1}{N}\sum_{i=1}^{N} (x_i - x_{curve}) \quad (1)$$

$$AARD = \sqrt{\frac{1}{N}\sum_{i=1}^{N} (x_i - x_{curve})^2} \quad (2)$$

This was done for both the heat of absorption data as well as CO_2 partial pressure data. For the heat of absorption the average deviation between the fitted curve and the experimental data (AD) was 1.6 kJ/mol_{CO2} and the average standard deviation (AARD) was 2.0 kJ/mol_{CO2}. For

partial pressure of CO_2 the average deviation was 1.3 kPa and the standard deviation was 1.9 kPa. The deviation between the repeated experiments, 1.6 kJ/mol$_{CO2}$ is in good agreement with the uncertainty for the differential heat of absorption (2.1%). Finally, the correct operation was ensured by measuring the heat of absorption of 30wt% MEA at 40°C. The data agree well with the data of Kim et al. (2014) with AD of 2.9 kJ/mol$_{CO2}$ for the whole loading range of 0.05-0.6 mol$_{CO2}$/mol$_{MEA}$ and 1.7 kJ/mol$_{CO2}$ for the loadings up to 0.5 mol$_{CO2}$/mol$_{MEA}$.

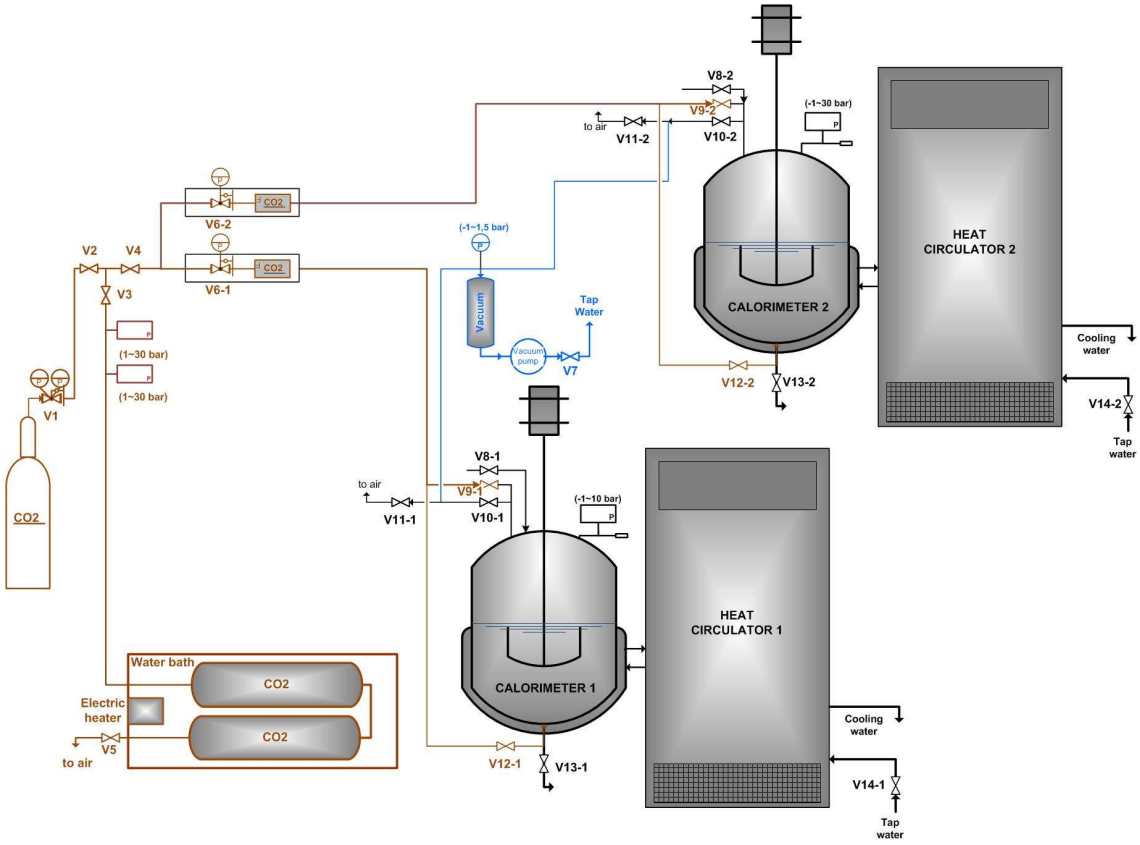

Figure 1 Calorimetric setup used in this work.

2.1 Calculation of the cyclic capacity

For post combustion CO_2 capture the flue gas typically contains 10-14 kPa CO_2, whereas for example in biogas upgrading the amount of CO_2 in the gas is often over 40 kPa. The partial pressure of CO_2 in the gas entering the absorption process will determine the maximum loading that can be theoretically reached. This is the loading that is in equilibrium with the partial pressure of CO_2 at the temperature at the bottom of the absorber. At regeneration temperatures (typically ~120°C) solvent systems with high CO_2 pressure are easier to strip even at low

loadings. Low partial pressure of CO_2 in the stripper makes it more energy demanding to regenerate the solvent to low lean loadings by increasing the stripping steam requirements. The larger cyclic capacity, the less solvent has to be pumped around.

In this work, the cyclic capacity was calculates as the difference between the rich and lean loading ($mol_{CO2}/L_{solution}$). At 40°C, CO_2 partial pressure of 9.5kPa was used to determine the rich loading. This is a CO_2 partial pressure used during rapid solvent screening for post combustion CO_2 capture by several authors (Aronu et al., 2014; Brúder et al., 2012; Hartono et al., 2017). In case of 30wt% MEA this choice of equilibrium pressure at 40°C, gives a rich loading of 0.5 mol_{CO2}/mol_{MEA} (Brúder et al., 2012). The partial pressure of CO_2 at 120°C giving the lean loading was chosen based on existing data on 30wt% MEA. 30wt% MEA is typically stripped down to loadings 0.2-0.25 mol_{CO2}/mol_{MEA} (Rabensteiner et al., 2016). Choosing loading 0.25 mol_{CO2}/mol_{MEA} gives partial pressure of 20kPa (Brúder et al., 2012). It is assumed that the DEEA+MAPA blends can be stripped down to the same CO_2 partial pressure at 120°C.

3. Results and discussion

Experiments were performed with five different solvent blends: *3M DEEA + 1.5M MAPA, 3M DEEA + 2M MAPA, 3M DEEA + 3M MAPA, 3M DEEA + 3.5M MAPA and 1M DEEA + 5M MAPA*. It is known that blends of DEEA and MAPA may form two liquid phases during absorption (Arshad et al., 2013; Ciftja et al., 2015; Pinto et al., 2014b). The formation of two liquid phases depends on the composition of the blend and the two phases that are formed may become one phase again above a certain CO_2 loading. After each experiment, the presence of two phases was visually observed at room temperature. Two phases were detected in the *3M DEEA + 3M MAPA* –blend after measurements at 40°C, 80°C and 120°C and *3M DEEA + 3.5M MAPA* –blend after experiments at 80°C and 120°C. However, the fact that two phases were observed at room temperature, does not necessary mean that two phases were present during the experiments. Furthermore, based on the data presented in this work, it is not known at what loading the two liquid phases are formed or are present.

3.1 Effect of MAPA concentration

In Figure 2 to Figure 4 the heat of absorption of CO_2 in blends of 3M DEEA and MAPA is shown at 40°C, 80°C and 120°C. *3M DEEA + 1.5M MAPA* shows the lowest heat of absorption of CO_2 at 40°C, 80°C and 120°C. Increasing the MAPA concentration to 2M, 3M and 3.5M, increases the heat of absorption at each temperature. The same trend can actually be seen in the data from Arshad et al. (2013) where the heat of absorption of CO_2 in blends of *5M*

DEEA+1M MAPA and *5M DEEA+2M MAPA* was studied: the increase of MAPA concentration from 1M to 2M in 5M DEEA increased the heat of absorption at low loadings.

It can also be noticed from Figure 2 to Figure 4 that the differential heat of absorption slowly decreases with increasing loading. For most of the systems the decrease is slow in the beginning before starting to decrease faster (typically between 0.4 and 0.5 mol_{CO2}/mol_{amine}). This is more visible for the systems with the highest MAPA concentrations. Finally, the heat of absorption is close to the heat of absorption of DEEA, around 60 kJ/mol_{CO2} (Arshad et al., 2013).

The formation of two phases, seen in *3M DEEA + 3M MAPA* at 40ºC, 80ºC and 120ºC, as well as at 80ºC and 120ºC in *3M DEEA + 3.5M MAPA* does not seem to have an effect on the heat of absorption of CO_2 or on the behavior of the partial pressure CO_2 curves. However, as discussed in the Introduction, the interest in operating systems forming two liquid phases is related to the regeneration of a smaller amount of liquid and the potential to operate in a loading range with a low heat of absorption (Pinto et al., 2014b). It should be noted that there is a small increase in the heat of absorption of CO_2 in *3M DEEA + 3M MAPA* system at 120ºC at loading $0.1 mol_{CO2}/mol_{amine}$. A similar increase is seen for *3M DEEA+ 1.5M MAPA* and *3M DEEA+2M MAP*A solutions with the same loading. But since this is not visible at other temperatures it is not believed to be related to the formation of two phases.

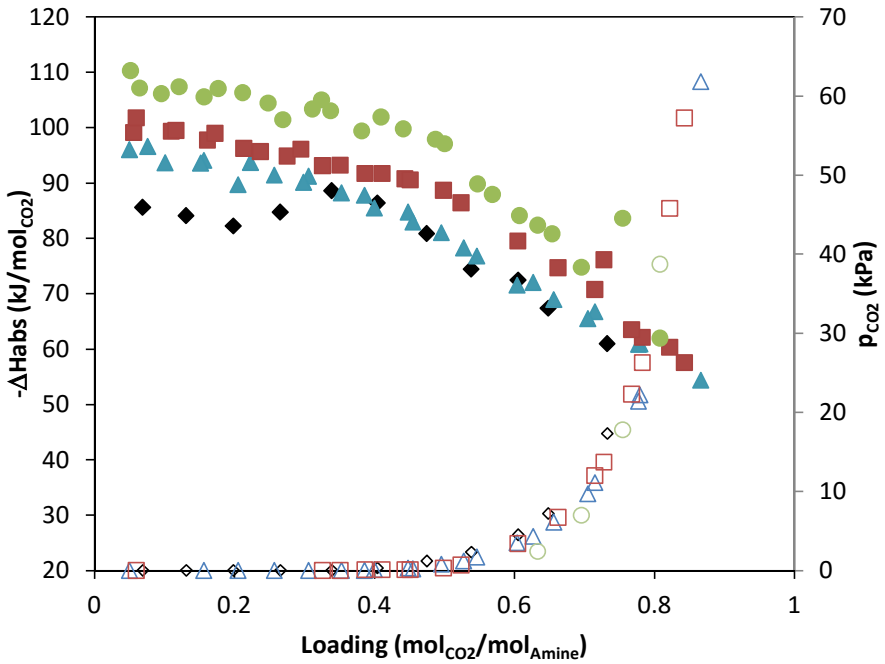

Figure 2. Heat of absorption (ΔHabs) of CO_2 and partial pressure of CO_2 in blends of 3M DEEA and 1-3.5M MAPA at 40°C. Closed markers are used for heat of absorption and open markers are used for partial pressure of CO_2. ●/○ 3M DEEA + 3.5M MAPA ; ■/□ ; 3M DEEA + 2M MAPA ; ▲/△ 3M DEEA + 2M MAPA; ◆/◇ 3M DEEA + 1.5M MAPA.

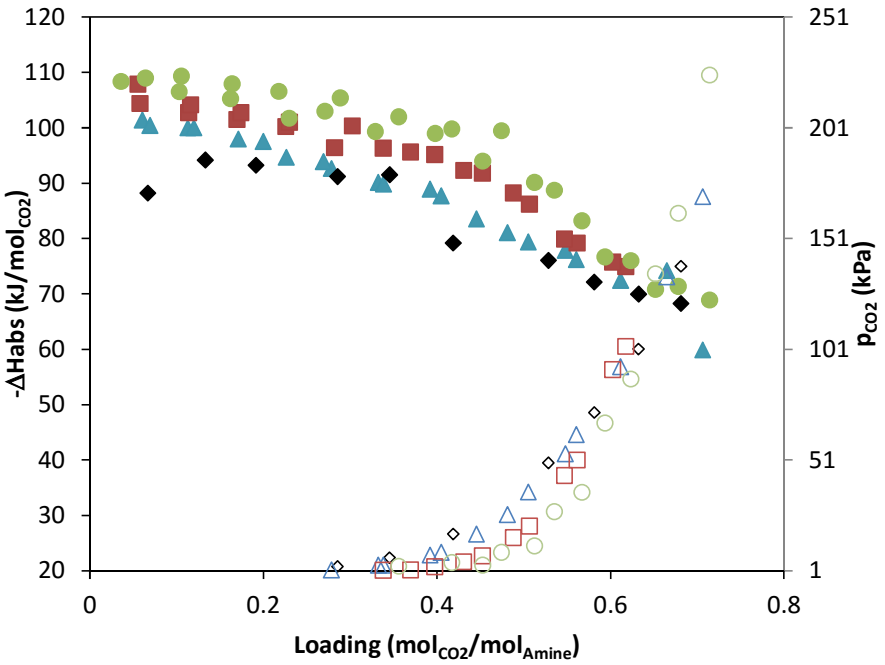

Figure 3 Heat of absorption (ΔHabs) of CO_2 and partial pressure of CO_2 in blends of 3M DEEA and 1-3.5M MAPA at 80°C. Closed markers are used for heat of absorption and open markers are used for partial pressure of CO_2. ●/○ 3M DEEA + 3.5M MAPA ; ■/□ ; 3M DEEA + 2M MAPA ; ▲/△ 3M DEEA + 2M MAPA; ◆/◇ 3M DEEA + 1.5M MAPA.

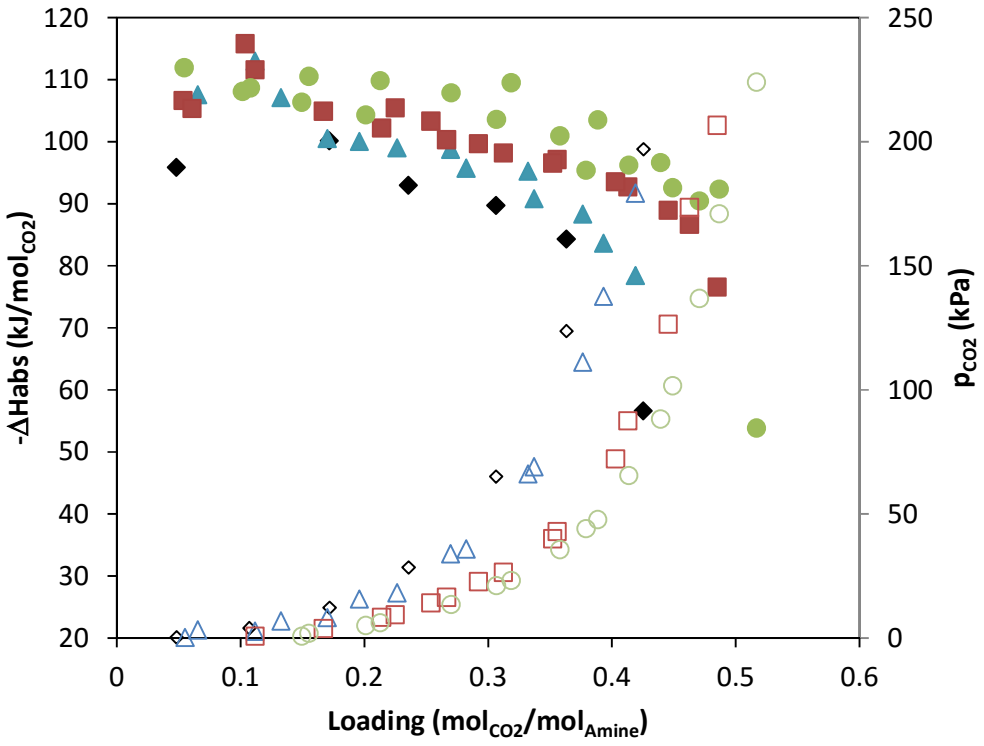

Figure 4 Heat of absorption (ΔHabs) of CO_2 and partial pressure of CO_2 in blends of 3M DEEA and 1-3.5M MAPA at 120°C. Closed markers are used for heat of absorption and open markers are used for partial pressure of CO_2. ●/○ 3M DEEA + 3.5M MAPA ; ■/□ ; 3M DEEA + 2M MAPA ; ▲/△ 3M DEEA + 2M MAPA; ◆/◇ 3M DEEA + 1.5M MAPA.

The heat of absorption values of *3M DEEA + 2M MAPA* can be compared to the literature values of *5M DEEA + 2M MAPA*. The behavior of the systems is very similar in mol_{CO2}/mol_{amine} basis, as shown in Figure 5. Even the "saturation point of MAPA" where DEEA starts to increasingly dominate the absorption causing a fast decline in the heat of absorption, is very similar (~0.3mol_{CO2}/mol_{amine} at 40°C). However, if the plot is made using mol_{CO2}/mol_{MAPA} or mol/L, the "saturation point" is not the same. This is illustrated also in Figure 5 where the plot based on mol_{CO2}/mol_{MAPA} is shown. If it was only the MAPA reaction with CO_2 in the beginning, one would expect the behavior of these different systems with same MAPA concentration present to be the same until almost all MAPA has reacted. However, this is not the case as also seen from Figure 5. It is clear that the heat of absorption of *5M DEEA + 2M MAPA* decreases less steeply and it also decreases later compared to the behavior of *3M DEEA + 2M MAPA* both at 40°C and 120°C. This indicates that the amount of DEEA present in the solution has an influence on the heat of absorption at least at higher loadings.

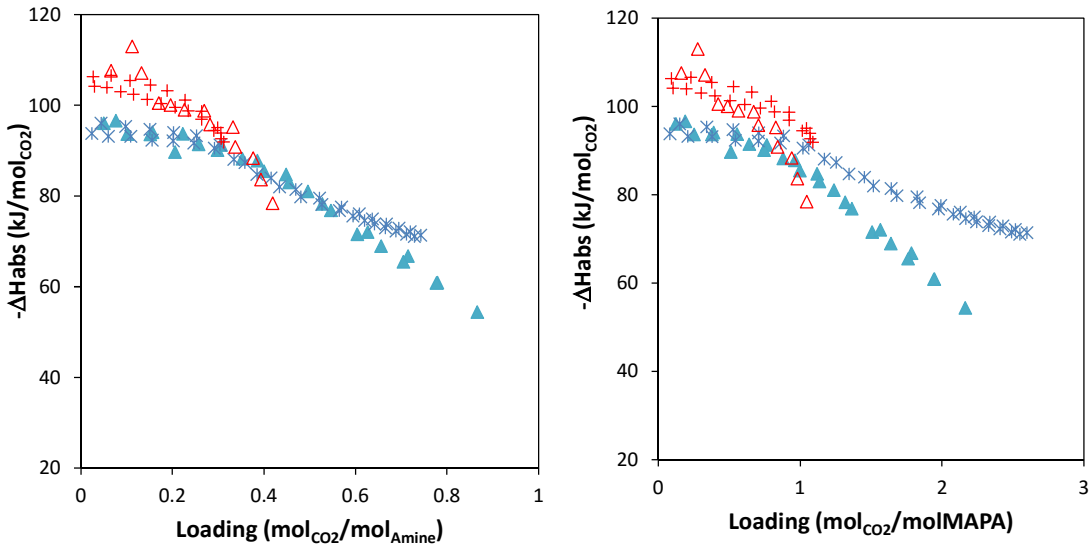

Figure 5 Heat of absorption of CO_2 in blends of 3M DEEA+2M MAPA and 5M DEEA+2M MAPA at 40°C and 120°C. On the left-hand side as a function of mol_{CO2}/mol_{Amine} and on the right-hand side mol_{CO2}/mol_{MAPA}. ▲3M DEEA + 2M MAPA at 40°C; △3M DEEA + 2M MAPA at 120°C; ✱ 5M DEEA + 2M MAPA at 40°C (Arshad et al., 2013); +5M DEEA + 2M MAPA at 120°C (Arshad et al., 2013).

Experiments were also performed with an aqueous blend of *1M DEEA+5M MAPA*. The heat of absorption of CO_2 in *1M DEEA+5M MAPA* was quite constant until high loadings ($0.8 mol_{CO2}/mel_{amine}$) at all temperatures, as shown in Figure 6. This is due to the high amount of MAPA, and the shape of curve is similar to those of 1M and 2M MAPA solutions reported in the literature (Arshad et al., 2013). Also here, the heat of absorption of CO_2 rises with increasing temperature. Looking at the data at 40°C, one can see that the heat of absorption of *1M DEEA+5M MAPA* is very close to that of *5M MAPA*. Both of these solutions have a higher heat of absorption compared to those of 1M and 2M MAPA showing that the heat of absorption is also a function of the amine concentration. In addition, the heat of absorption of CO_2 of *1M DEEA + 5M MAPA* is less temperature dependent than 1M and 2M MAPA solutions; at 40°C the heat of absorption of CO_2 in *1M DEEA+5M MAPA* is higher than *1M* and *2M MAPA* whereas at 120°C the order is the opposite. Two possible reasons could be considered: It could be due to the effect of DEEA or it could be related to the differences in the experimental method. Arshad et al. (2013) fed the CO_2 into the gas phase, whereas in the current work CO_2 was added directly into the liquid phase. Kim et al. (2014) reported that feeding the CO_2 directly into the liquid phase decreased the temperature dependency of the heat of absorption of CO_2 in the case of 30wt% MEA.

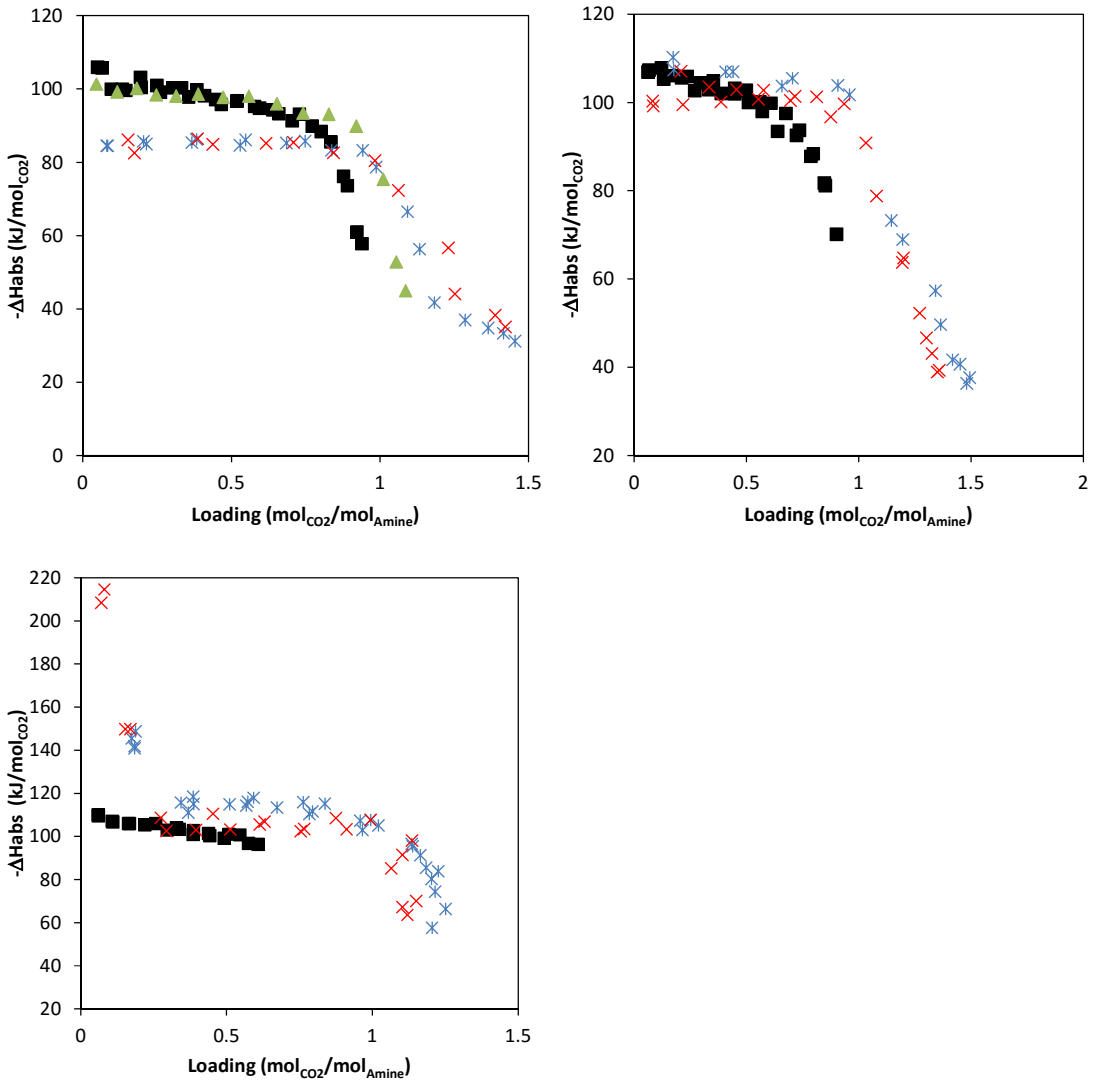

Figure 6 Heat of absorption of CO_2 in 1M DEEA + 5M MAPA, 1M MAPA, 2M MAPA and 5M MAPA at 40°C(upper left-hand corner), 1M DEEA + 5M MAPA, 1M MAPA and 2M MAPA at 80°C (upper right-hand corner) and 1M DEEA + 5M MAPA, 1M MAPA, 2M MAPA at 120°C (lower left-hand corner). ■ 1M DEEA + 5M MAPA ; ▲ 5M MAPA (in-house data); ✳1M MAPA (Arshad et al., 2013) ; ×2M MAPA (Arshad et al., 2013)

Looking at all the systems studied in this work, the heat of absorption of CO_2 in different blends of DEEA-MAPA and single amine MAPA solutions is plotted in Figure 7 at 40°C and loading 0.2mol$_{CO2}$/mol$_{amine}$. The temperature of 40°C was chosen due to relative constant heat of absorption at low loadings for most of the systems, and the loading of 0.2mol$_{CO2}$/mol$_{amine}$ was chosen to avoid the high initial heat of absorption values reported often in the literature. However, higher loading could have been used in the figure. The figure indicates that heat of absorption in the blends of MAPA with 3M DEEA and 5M DEEA rises with increasing MAPA concentration. Similarly, in the case of MAPA-solution (~1M, 2M and 5M MAPA) the

differential heat of absorption has a concentration dependency. However, this dependency is somewhat lower compared to DEEA/MAPA–blends. The solution of *1M DEEA+5M MAPA,* agrees very well with the single *5M* MAPA solution which shows a lower value for the heat of absorption of CO_2 compared to that of *3M DEEA+3M MAPA*. The results overall indicate that there are interactions between the DEEA and MAPA influencing the heat of absorption of CO_2. These interactions appear to be dependent, at least, on the concentration of MAPA in the blend. A rigorous thermodynamic model that is able to predict the speciation and activities in the liquid phase could perhaps help to explain some of the results on more fundamental level.

Furthermore, in the literature it has been proposed that mixtures of two solvents with different heats of absorption would give an "averaged" heat of absorption. Several investigators have already found that this postulation is not valid for amine mixtures (Arshad et al., 2013; Kim and Svendsen, 2011) and newer results further support this. The heat of absorption of a single MAPA system at 40°C has been reported to be around 84 kJ/mol for MAPA (1M and 2M solutions) and around 60 kJ/mol for 5M DEEA (Arshad et al., 2013). In this current work a higher heat of absorption than that in the single MAPA system is seen. The same can be seen in the data by Arshad et al. (2013) in the case of *5M DEEA+2M MAPA*; up to loading $0.3 mol_{CO2}/mol_{amine}$ the heat of absorption is higher than that of aqueous 2M MAPA.

As a final point, the current results also clearly show that the heat of absorption of CO_2 in the studied amine blends is a function of temperature and CO_2 content in the liquid phase. This is in agreement with the literature, where same has been reported for several solvent systems (Arshad et al., 2013; Kim and Svendsen, 2011; Svensson et al., 2014).

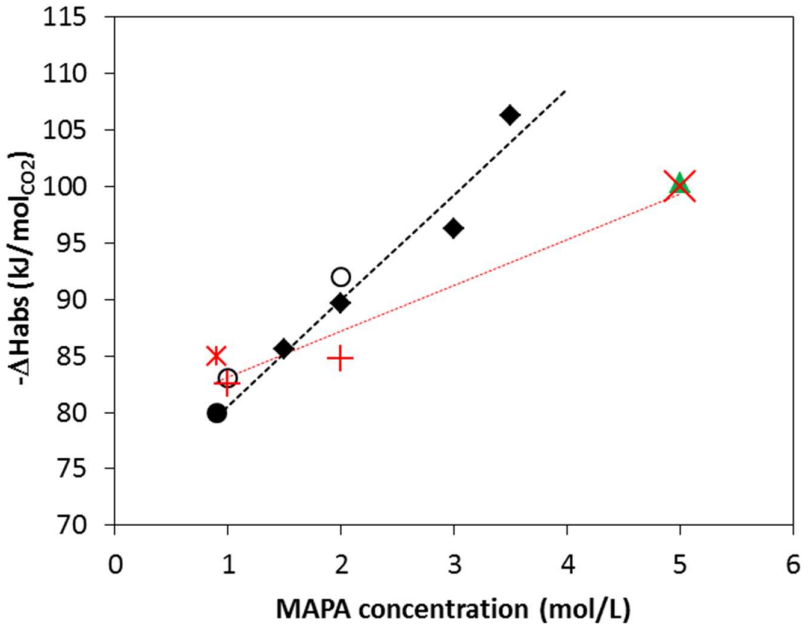

Figure 7 Heat of absorption of CO_2 at loading 0.2mol_{CO2}/mol_{amine} at 40°C. ○ 5M DEEA + MAPA blends (Arshad et al., 2013); ◆ 3M DEEA + MAPA blends (this work); ● 3M DEEA + 0.9M MAPA (Kim and Svendsen, 2011); + MAPA solutions (Arshad et al., 2013); ✳0.9M MAPA (Kim and Svendsen, 2011); ×5M MAPA (in-house data) ▲ 1M DEEA+5M MAPA (this work).

3.2 Absorption capacity

The absorption capacity of the solvent was estimated using the equilibrium curves of CO_2. In the absorber it is beneficial to have a solvent system where the partial pressure of CO_2 starts to increase as high loading as possible. Using the partial pressure of CO_2 data shown in Figure 2-Figure 6, at 40°C and 120°C, the cyclic capacity was calculated for the studied systems. At 40°C, CO_2 partial pressure of 9.5kPa was used to determine the rich loading. At 120°C, CO_2 pressure of 20 kPa was used.

The results are given in Figure 8. It can be seen that all the studied systems revealed higher cyclic capacity compared to that of 30wt% MEA. In the case of the 3M DEEA–family, the increase of MAPA concentration increases the cyclic capacity and *3M DEEA + 3.5M MAPA* shows the highest cyclic capacity. As seen in Figure 2, the CO_2 partial pressure curves almost overlap at ~10 kPa giving very similar rich loadings to all the blends with 3M DEEA. Even though the lean loadings are somewhat more different (Figure 4), overall it can be concluded that, the rich and lean loadings (mol_{CO2}/mol_{amine}) are fairly similar and the difference in cyclic capacity comes from the total amine concentration. Even though the increase in the MAPA concentration increases the cyclic capacity in 3M DEEA solutions, the *1M DEEA + 5M MAPA* has only 80% of the cyclic capacity of *3M DEEA + 3.5M MAPA*. *1M DEEA + 5M MAPA* –system can absorb CO_2 up to loading close to 1 mol_{CO2}/mol_{amine} at 40°C but the equilibrium at 120°C is less favorable for CO_2 stripping limiting the lean loading. In case of the 3M DEEA solutions, both the cyclic capacity (mol_{CO2}/L) and the heat of absorption rises with increasing MAPA concentration as can be seen when comparing, for example, Figure 7 and Figure 8. However, 1M DEEA + 5M MAPA has the second highest heat of absorption (Figure 7) but has cyclic capacity close to that of 3M DEEA + 1.5M MAPA.

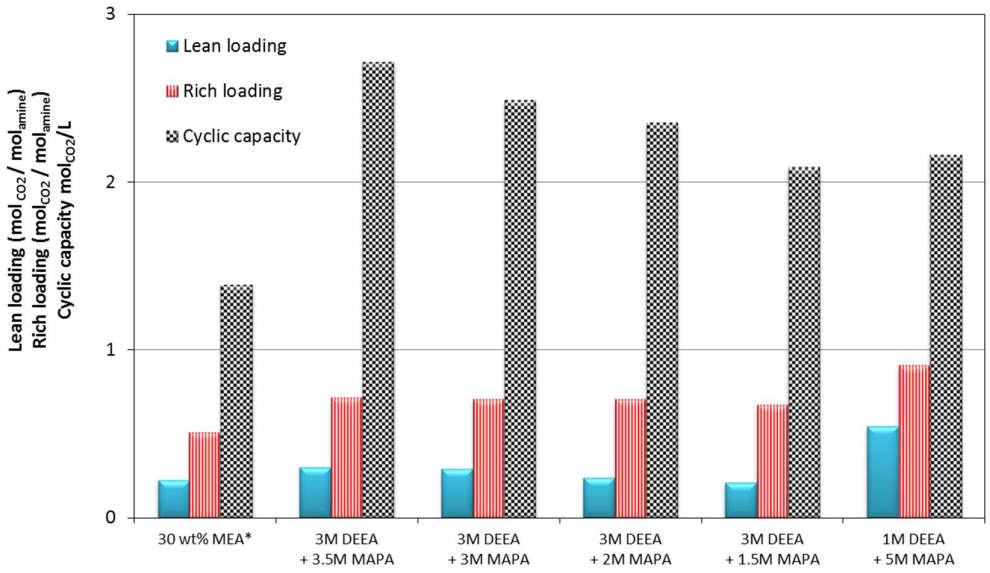

Figure 8 Cyclic capacity of the studied solvent systems based on partial pressure of CO_2 at 40°C (9.5kPa) and 120°C (20kPa). *30wt% MEA is calculated using model in Brúder et al. (2012).

4. Conclusions

In this work the heat of absorption of CO_2 in aqueous blends of DEEA+MAPA solutions was measured as a function of CO_2 loading at 40°C, 80°C and 120°C. The partial pressure of CO_2 was also estimated from the total pressure measurements. The main motivation was to study the effect of the MAPA concentration on the heat of absorption and the results found that increasing the concentration of MAPA in 3M DEEA solution increased the heat of absorption at all temperatures. Furthermore, solutions with a high amount of MAPA (5M) and a small amount of DEEA (1M) show qualitative behavior that is close to that of the aqueous 5M MAPA solution. Cyclic capacity calculated using the partial pressure of CO_2 showed that in blends containing 3M DEEA and varying amounts of MAPA, the cyclic capacity rose with an increasing MAPA concentration.

ACKNOWLEDGMENTS

Financial support from The Research Council of Norway through project 3GMC (3rd Generation Solvent Membrane Contactor, Project No. 239789), is gratefully acknowledged. Inna Kim is acknowledged for the technical support.

References

Aronu, U.E., Kim, I., Haugen, G., 2014. Evaluation of Energetic Benefit for Solid-liquid Phase Change CO2 Absorbents. Energy Procedia 63, 532-541.

Arshad, M.W., Fosbøl, P.L., von Solms, N., Svendsen, H.F., Thomsen, K., 2013. Heat of Absorption of CO2 in Phase Change Solvents: 2-(Diethylamino)ethanol and 3-(Methylamino)propylamine. Journal of Chemical & Engineering Data 58, 1974-1988.
Brúder, P., Lauritsen, K.G., Mejdell, T., Svendsen, H.F., 2012. CO2 capture into aqueous solutions of 3-methylaminopropylamine activated dimethyl-monoethanolamine. Chemical Engineering Science 75, 28-37.
Ciftja, A.F., Svendsen, H.F., Knuutila, H.K., 2015. Two phase formation and cyclic capacity of DEEA-MAPA blends, 8th Trondheim Conference on CO2 Capture, Transport and Storage TCCS-8, Trondheim.
Hartono, A., Vevelstad, S.J., Ciftja, A., Knuutila, H.K., 2017. Screening of strong bicarbonate forming solvents for CO2 capture. International Journal of Greenhouse Gas Control 58, 201-211.
Jonassen, Ø., Kim, I., Svendsen, H.F., 2014. Heat of Absorption of Carbon Dioxide (CO2) into Aqueous N-Methyldiethanolamine (MDEA) and N,N-Dimethylmonoethanolamine (DMMEA). Energy Procedia 63, 1890-1902.
Kim, I., Hoff, K.A., Mejdell, T., 2014. Heat of Absorption of CO2 with Aqueous Solutions of MEA: New Experimental Data. Energy Procedia 63, 1446-1455.
Kim, I., Svendsen, H.F., 2007. Heat of Absorption of Carbon Dioxide (CO2) in Monoethanolamine (MEA) and 2-(Aminoethyl)ethanolamine (AEEA) Solutions. Industrial & Engineering Chemistry Research 46, 5803-5809.
Kim, I., Svendsen, H.F., 2011. Comparative study of the heats of absorption of post-combustion CO2 absorbents. International Journal of Greenhouse Gas Control 5, 390-395.
Liebenthal, U., Pinto, D.D.D., Monteiro, J.G.M.S., Svendsen, H.F., Kather, A., 2013. Overall Process Analysis and Optimisation for CO2 Capture from Coal Fired Power Plants based on Phase Change Solvents Forming Two Liquid Phases. Energy Procedia 37, 1844-1854.
Liu, J., Wang, S., Svendsen, H.F., Idrees, M.U., Kim, I., Chen, C., 2012. Heat of absorption of CO2 in aqueous ammonia, piperazine solutions and their mixtures. International Journal of Greenhouse Gas Control 9, 148-159.
Merkley, K.E., Christensen, J.J., Izatt, R.M., 1986. Enthalpies of solution of CO2 in aqueous methyldiehtanolamine solutions. RR-102, , in: Report, G.R. (Ed.). Brigham Young University, Provo, UT.
Monteiro, J.G.M.S., Knuutila, H., Penders-van Elk, N.J.M.C., Versteeg, G., Svendsen, H.F., 2015. Kinetics of CO2 absorption by aqueous N,N-diethylethanolamine solutions: Literature review, experimental results and modelling. Chemical Engineering Science 127, 1-12.
Monteiro, J.G.M.S., Pinto, D.D.D., Luo, X., Knuutila, H., Hussain, S., Mba, E., Hartono, A., Svendsen, H.F., 2013. Activity-based Kinetics of the Reaction of Carbon Dioxide with Aqueous Amine Systems. Case Studies: MAPA and MEA. Energy Procedia 37, 1888-1896.
Pinto, D.D.D., Knuutila, H., Fytianos, G., Haugen, G., Mejdell, T., Svendsen, H.F., 2014a. CO2 post combustion capture with a phase change solvent. Pilot plant campaign. International Journal of Greenhouse Gas Control 31, 153-164.
Pinto, D.D.D., Zaidy, S.A.H., Hartono, A., Svendsen, H.F., 2014b. Evaluation of a phase change solvent for CO2 capture: Absorption and desorption tests. International Journal of Greenhouse Gas Control 28, 318-327.
Rabensteiner, M., Kinger, G., Koller, M., Hochenauer, C., 2016. Pilot plant study of aqueous solution of piperazine activated 2-amino-2-methyl-1-propanol for post combustion carbon dioxide capture. International Journal of Greenhouse Gas Control 51, 106-117.
Svensson, H., Zejnullahu Velasco, V., Hulteberg, C., Karlsson, H.T., 2014. Heat of absorption of carbon dioxide in mixtures of 2-amino-2-methyl-1-propanol and organic solvents. International Journal of Greenhouse Gas Control 30, 1-8.

APPENDIX

Table A1. Heat of absorption of CO_2 and partial pressure of CO_2 in 3M DEEA + 1.5M MAPA As a function of loading.

Loading	- DHabs		pCO2	Loading	- DHabs		pCO2
mol_{CO2}/mol_{MEA}	kJ/mol CO_2	kJ/mol-Amine	kPa	mol_{CO2}/mol_{MEA}	kJ/mol CO_2	kJ/mol-Amine	kPa
40 °C				**80 °C**			
0.07	85.60	5.94		0.07	88.10	5.88	
0.13	84.11	11.14		0.13	94.13	12.12	
0.20	82.22	16.70		0.19	93.16	17.58	0.1
0.27	84.72	22.37		0.29	91.12	26.14	2.8
0.34	88.62	28.90		0.35	91.46	31.62	6.8
0.40	86.36	34.53	0.3	0.42	79.14	37.43	17.5
0.48	80.86	40.22	1.2	0.53	75.96	45.76	49.6
0.54	74.42	44.94	2.3	0.58	72.07	49.56	72.4
0.61	72.45	49.80	4.5	0.63	69.90	53.12	101.1
0.65	67.39	52.70	7.2	0.68	68.17	56.46	138.4
0.73	60.97	57.84	17.3				
120 °C							
0.05	95.84	4.63	0.3				
0.11	108.72	11.02	4.0				
0.17	100.14	17.52	12.3				
0.24	92.98	23.47	28.4				
0.31	89.74	29.79	65.1				
0.36	84.28	34.59	123.8				
0.43	56.57	38.11	197.0				

Table A2. Heat of absorption of CO_2 and partial pressure of CO_2 in 3M DEEA + 2M MAPA As a function of loading.

Loading	- DHabs		pCO2	Loading	- DHabs		pCO2
mol_{CO2}/mol_{MEA}	kJ/mol CO_2	kJ/mol-Amine	kPa	mol_{CO2}/mol_{MEA}	kJ/mol CO_2	kJ/mol-Amine	kPa
40 °C				**80 °C**			
0.05	96.02	4.84		0.06	101.34	6.10	
0.10	93.61	9.63		0.11	99.95	11.37	
0.16	94.05	14.80		0.17	97.91	17.05	
0.21	89.68	19.20		0.23	94.59	22.29	0.1
0.26	91.40	23.94		0.28	92.56	27.10	1.1
0.31	91.23	28.41		0.33	90.08	31.97	3.28
0.35	88.24	32.51		0.39	88.87	37.27	7.9

0.40	85.48	36.55	0.1	0.45	83.49	41.74	17.3
0.45	84.75	40.66	0.3	0.51	79.33	46.47	36.3
0.50	81.03	44.51	0.8	0.56	76.10	50.70	62.3
0.55	76.80	48.40	1.7	0.61	72.35	54.39	92.9
0.60	71.55	52.49	3.5	0.66	74.16	58.33	133.6
0.66	68.91	56.10	6.1	0.71	59.84	60.81	169.7
0.72	66.75	60.02	11.1	0.07	100.35	6.95	
0.78	60.87	63.94	22.2	0.12	99.93	12.00	
0.87	54.35	68.67	61.8	0.20	97.44	19.81	
0.08	96.57	7.41		0.27	93.83	26.30	0.5
0.15	93.59	14.44		0.34	89.74	32.52	3.3
0.22	93.70	21.12		0.40	87.63	38.34	9.1
0.30	90.12	27.95		0.48	80.99	44.52	26.2
0.39	87.76	35.60		0.55	77.84	49.72	53.6
0.46	82.95	41.36	0.2	**120 °C**			
0.53	78.28	47.01	1.2	0.11	112.98	9.23	2.7
0.63	72.02	54.15	4.3	0.17	100.51	15.09	8.1
0.71	65.49	59.28	9.7	0.23	99.00	20.67	18.1
0.78	60.84	63.69	21.4	0.28	95.72	26.03	35.8
				0.34	90.78	31.01	68.9
				0.39	83.62	35.70	137.6
				0.07	107.55	7.06	3.2
				0.13	107.09	14.25	6.8
				0.20	100.02	20.61	15.6
				0.27	98.75	27.87	33.9
				0.33	95.22	33.83	66.0
				0.38	88.32	37.75	111.2
				0.42	78.39	41.07	179.3

Table A3. Heat of absorption of CO_2 and partial pressure of CO_2 in 3M DEEA + 3M MAPA As a function of loading.

Loading	- DHabs		pCO2	Loading	- DHabs		pCO2
mol_{CO2}/mol_{MEA}	kJ/mol CO_2	kJ/mol-Amine	kPa	mol_{CO2}/mol_{MEA}	kJ/mol CO_2	kJ/mol-Amine	kPa
40 °C				**80 °C**			
0.06	99.11	5.59		0.06	104.37	6.03	
0.11	99.33	10.91		0.11	102.73	11.80	
0.16	97.74	15.96		0.17	101.47	17.43	
0.21	96.27	20.93		0.23	100.23	23.09	
0.28	94.86	26.83		0.28	96.41	28.51	0.3
0.33	93.09	31.52		0.34	96.27	33.89	1.1

0.39	91.69	37.07	0.1	0.40	95.15	39.54	2.7
0.44	90.75	42.25	0.1	0.45	91.81	44.60	7.7
0.50	88.64	47.16	0.3	0.51	86.17	49.26	21.1
0.73	76.13	64.60	13.7	0.56	79.19	53.61	51.0
0.78	62.10	68.00	26.3	0.62	74.90	57.80	102.2
0.84	57.55	71.46	57.2	0.06	107.87	5.97	
0.06	101.76	6.08		0.12	104.12	12.29	
0.12	99.48	11.70		0.17	102.71	18.27	
0.17	98.97	17.25		0.23	101.00	23.90	
0.24	95.69	23.43		0.30	100.30	31.18	
0.29	96.09	28.99		0.37	95.62	37.58	1.3
0.35	93.20	34.21		0.43	92.26	43.24	5.0
0.41	91.68	39.73	0.1	0.49	88.21	48.28	15.9
0.45	90.56	43.37	0.1	0.55	79.91	53.01	44.0
0.52	86.41	49.63	0.7	0.60	75.73	57.20	91.7
0.60	79.51	56.09	3.4	**120 °C**			
0.66	74.66	60.37	6.7	0.05	106.63	5.71	
0.71	70.76	64.10	12.0	0.10	115.80	11.52	
0.77	63.51	67.42	22.3	0.22	105.44	24.29	9.4
0.82	60.33	70.70	45.8	0.27	100.33	28.46	16.4
				0.31	98.19	32.98	26.4
				0.36	97.12	37.19	42.8
				0.41	92.74	42.50	87.5
				0.46	86.68	46.81	173.4
				0.06	105.36	6.39	
				0.11	111.59	12.09	0.6
				0.17	104.91	17.89	3.8
				0.21	102.20	22.70	8.3
				0.25	103.33	26.81	14.1
				0.29	99.68	30.63	22.6
				0.35	96.56	36.42	39.9
				0.40	93.56	41.17	72.1
				0.45	88.93	44.96	126.4
				0.49	76.56	47.99	206.6

Table A4. Heat of absorption of CO_2 and partial pressure of CO_2 in 3M DEEA + 3.5M MAPA As a function of loading.

Loading	- DHabs		pCO2	Loading	- DHabs		pCO2
mol_{CO2}/mol_{MEA}	kJ/mol CO_2	kJ/mol-Amine	kPa	mol_{CO2}/mol_{MEA}	kJ/mol CO_2	kJ/mol-Amine	kPa
40 °C				**80 °C**			
0.05	110.26	5.7		0.57	83.17	56.42	36.3
0.10	106.11	10.4		0.62	75.98	60.70	87.5
0.16	105.51	16.8		0.68	71.33	64.60	162.4
0.21	106.32	22.7		0.71	68.85	67.09	224.7

0.27	101.41	28.5	
0.32	105.00	34.3	
0.38	99.41	40.0	
0.44	99.79	45.9	
0.50	97.05	51.6	
0.57	87.95	57.6	
0.63	82.34	63.0	2.4
0.70	74.76	67.6	7.0
0.75	83.60	72.6	17.8
0.81	61.97	75.9	38.7
0.06	107.14	6.9	
0.12	107.40	13.0	
0.18	107.03	19.0	
0.25	104.42	26.4	
0.31	103.34	32.9	
0.34	103.03	35.6	
0.41	101.91	43.0	
0.49	97.88	50.6	
0.55	89.81	56.0	
0.61	84.11	61.0	
0.65	80.83	64.8	
80 °C			
0.06	108.99	6.97	
0.10	106.48	11.12	
0.16	105.22	17.34	
0.22	106.53	23.26	
0.27	102.96	28.74	
0.33	99.31	34.53	
0.40	98.98	41.34	0.9
0.45	94.00	46.49	3.4
0.51	90.08	51.87	12.1

0.04	108.35	3.89	0.2
0.11	109.31	11.48	
0.16	107.90	17.80	
0.23	101.72	24.50	
0.29	105.38	30.70	0.4
0.36	101.96	37.58	3
0.42	99.77	43.68	4.7
0.47	99.45	49.37	9.2
0.54	88.68	54.77	27.6
0.59	76.66	59.24	67.7
0.65	70.79	63.37	135
120 °C			
0.05	111.93	6.09	
0.11	108.68	11.91	
0.15	106.37	16.32	0.6
0.20	104.31	21.72	5
0.31	103.59	32.65	21.1
0.36	100.92	37.82	35.6
0.38	95.36	39.85	44
0.41	96.22	43.17	65.5
0.45	92.56	46.44	101.6
0.47	90.42	48.40	136.8
0.05	134.14	6.80	
0.10	108.12	12.30	
0.16	110.52	18.24	1.9
0.21	109.83	24.55	6.1
0.27	107.87	30.75	13.4
0.32	109.50	36.06	23.1
0.39	103.49	43.31	47.7
0.44	96.64	48.20	88.2
0.49	92.33	52.58	170.9
0.52	53.83	54.19	224

Table A5. Heat of absorption of CO_2 and partial pressure of CO_2 in 1M DEEA + 5M MAPA As a function of loading.

Loading	- DHabs		pCO2	Loading	- DHabs		pCO2
mol_{CO2}/mol_{MEA}	kJ/mol CO_2	kJ/mol-Amine	kPa	mol_{CO2}/mol_{MEA}	kJ/mol CO_2	kJ/mol-Amine	kPa
40 °C				**80 °C**			
0.05	105.87	5.29		0.56	100.15	58.47	2
0.10	99.94	9.92		0.61	99.81	63.58	2.8
0.14	99.58	14.71		0.68	97.53	70.06	4.6
0.20	100.37	19.95		0.74	93.70	75.68	8.2

0.25	100.90	25.30	
0.30	100.28	30.69	
0.36	97.79	35.90	
0.41	98.14	41.07	
0.47	95.74	46.53	
0.52	96.69	51.54	0.1
0.58	95.20	57.24	0.1
0.64	94.20	63.07	0.3
0.70	91.26	68.98	0.3
0.77	89.83	75.06	0.5
0.84	85.49	80.44	1.2
0.89	73.55	84.51	5
0.92	60.96	86.47	12.4
0.06	105.72	6.85	
0.13	99.90	13.65	0.7
0.19	103.16	19.98	0.7
0.26	99.11	26.55	0.7
0.33	100.26	33.72	0.8
0.38	99.70	38.86	0.9
0.45	97.07	45.05	1
0.52	96.69	52.06	1
0.59	94.77	59.13	1
0.66	93.18	65.25	1.2
0.73	93.10	71.68	1.3
0.80	88.34	78.13	1.6
0.88	76.12	83.85	4.6
0.94	57.75	87.42	21.5

80 °C

0.07	107.32	7.15	
0.12	107.82	13.06	
0.18	106.07	18.87	
0.24	105.93	25.26	
0.30	104.42	31.44	0.3
0.35	104.86	37.51	0.5
0.45	103.21	47.26	1
0.50	102.76	52.64	1.4

0.80	88.37	81.15	18
0.85	81.72	85.16	39.8
0.06	106.88	6.65	
0.13	105.30	13.99	
0.21	105.58	22.48	
0.27	102.69	28.47	
0.33	102.93	34.77	
0.39	102.04	40.56	
0.45	101.97	46.70	
0.51	100.01	52.81	0.2
0.57	97.94	58.80	0.7
0.64	93.45	65.16	1.7
0.72	92.53	72.90	5.8
0.79	87.80	78.63	14.1
0.85	81.14	83.75	40.2
0.90	70.14	87.35	103.5

120 °C

0.06	109.44	6.64	
0.11	107.08	11.81	
0.17	105.90	18.03	
0.26	105.86	27.59	
0.30	102.93	31.60	
0.34	103.25	35.75	
0.39	102.69	40.94	2
0.44	100.32	46.43	5.9
0.51	100.95	53.09	13.4
0.58	96.68	59.65	26.4
0.06	109.96	6.64	
0.11	106.63	12.04	
0.16	105.90	17.74	
0.22	105.29	23.55	
0.27		28.03	
0.33	104.08	33.89	
0.39	100.85	39.65	1.1
0.44	101.30	44.92	4.6
0.49	99.09	50.27	10.3
0.55	100.65	55.71	19.1
0.61	96.29	61.75	36.1